

Detect Formation of Cavitation in Pump

Thammasak Thamma¹ Wanchai Asvapoositkul²
Department of Mechanical Engineering, Faculty of Engineering,
King Mongkut's University of Technology Thonburi,
91 Prachautid Tungkru Bangmod Bangkok 10140

Tel: +662-470-9123 Fax: +662-470-9111, E-mail: tma559@yahoo.com¹, wanchai.asv@kmutt.ac.th²

ABSTRACT

This paper presents numerical simulation of the cavitation in an axial flow pump impeller of high specific speed (NS 3.88). The study was carried out with a commercial Computational Fluid Dynamics (CFD) code (CFX TASCflow). The numerical simulation was conducted in order to study the cause of cavitation with respect to detect and analyze cavitation flow through an axial flow pump impeller. The onset of cavitation in term of the (impeller) discharge head, three percent Net Positive Suction Head (NPSH) head drop have been presented. The computed pump head, pressure distribution on the blade and rate of vapor production at difference NPSH value are computed to clarify the cavitation behavior. The cavitation model used is base on Volume of Fluid (VOF) model. The impeller is designed and developed using Force Vortex theory and design parameter (Stepanoff). The computational grid was generated by CFX-Turbogrid with H-Grid through the blade and flow passage. The total pressure at inflow boundary is reduced in small increments to meet the onset of cavitation. The CFD results computed by CFX-TASCFlow can be shown that the formation bubble form in a lower pressure area which caused by high velocity fluid. Inception cavitation occurs on the blade surface where the leading edge meets the tip. For lower NPSH values the cavitation zones move from leading to trailing edge. The drop in the head-NPSH curve begins when the cavity length is reached the maximum chord length of the blade.

NOMENCLATURE

\dot{m}_V	total interphase mass transfer rate per unit volume
N	bubbles per unit volume
NPSH _{3%}	three percent head drop net positive suction head
P ₁	inlet static pressure
P _{t1}	inlet absolute total pressure
P _{t2}	outlet absolute total pressure
R _B	bubble radius
S _{y,i}	source term of component i

V _B	bubble volume
\vec{V}_{circ}	circumferential plane velocity
\vec{V}_{merid}	meridional velocity
y	mass fraction
α	volume fraction

INTRODUCTION

Computational Fluid Dynamics (CFD) is a powerful tool which can be used in evaluating and predicting incipient cavitation because several cavitation models have been developed. In this paper, Volume of Fluid (VOF) model has been used to clarify occurrence of cavitation in a flow passage of an axial flow pump. A cavitation model has been implemented based on the use of the Rayleigh Plesset Equation to estimate the rate of vapor production.

The aim of this paper is to present results obtained with CFX TASCflow predicting inception cavitation as well as generation of vapor bubble. From this results, formation of cavitation has been examined in term of the (impeller) discharge head, three percent Net Positive Suction Head (NPSH). Several variable fringe plot on blade to blade view of inception cavitation are plotted to analyzed generation of vapor bubble. Location of maximum formation cavitation rate on the blade surface while NPSH reduced can be presented in this study.

An axial flow pump model in numerical simulation is characterized by a heigh specific speed (NS 3.88). At operating design point develops flow rate of 18 kg/s, head of 1.83 m at speed of 252 rad/s. The geometric blade impeller model is transferred to CFX TurboGrid that is used to generate computational grid. Flow through a blade passage is simulate to predic incipient cavitation. The numerical simulation results have been discussed to explain generation of vapor bubble and cavitation phenomenon that happen through the flow passage of axial flow pump.

Cavitation Model

VOF model is used to simulate flow with cavitation when local pressure decrease below vapor pressure. It is an effective model that used in CFX TASCflow [1]. This model applied Rayleigh-Plesset (RP) equation with the assumption that thermal and mechanical equilibrium exists between the phases. The RP equation provides the basis for the rate equation controlling vapor generation and construction that can be solved by a volume of fluid (VOF) volume fraction with source term.

The general advection-diffusion equation for the mass fraction of an individual component is given by [1]

$$\frac{\partial}{\partial t}(\rho y_i) + \frac{\partial}{\partial x_j}(\rho u_j y_i) = \frac{\partial}{\partial x_j} \left(\Gamma_{i,eff} \frac{\partial y_i}{\partial x_j} \right) + S_{y,i} \quad (1)$$

The mass fraction conservation equation transformed to terms of a volume fraction equation as shown below

$$\frac{\partial}{\partial t}(\rho_i \alpha_i) + \frac{\partial}{\partial x_j}(\rho_i u_j \alpha_i) = S_{\alpha,i} \quad (2)$$

To compute the rate of vapor generation and condensation, Rayleigh-Plesset has been used to derive source term. The rate of vaporization is given by

$$\dot{m}_v = N \rho_g \frac{dV_B}{dt} \quad (3)$$

and the rate of change of bubble volume is

$$\frac{dV_B}{dt} = \frac{d}{dt} \left(\frac{4}{3} \pi R_B^3 \right) \quad (4)$$

The Rayleigh Plesset equation describing the growth of a gas bubble in liquid is given by

$$R_B \frac{d^2 R_B}{dt^2} + \frac{3}{2} \left(\frac{dR_B}{dt} \right)^2 + \frac{2\sigma}{R_B} = \frac{p_v - p}{\rho_l} \quad (5)$$

where R_B represents the bubble diameter, p_v is the pressure in the bubble, p is the pressure in the liquid surrounding the bubble and σ is the surface tension coefficient between the liquid and vapor.

PUMP DESIGN

The axial flow pump showed in figure 1 is designed and developed using force vortex theory and design parameter (Stepanoff) [2]. Number of blade is assumed after solidity and hub ratio are chosen from design parameters. The speed constant of 0.5 is applied to the design of axial flow pump. Therefore, the impeller vane profiles are drawn from calculated inlet blade angle and outlet blade angle.

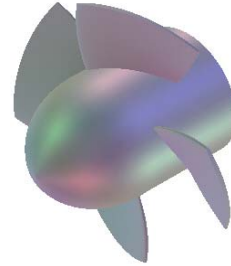


Figure 1 Axial Flow impeller (NS = 3.88)

Axial flow pump designed for this study, design operating run at 2400 rpm, a specific speed of 3.88, a rate flow of 18 kg/s and a head of 1.83 m. The blade geometries are described in Table 1.

Table 1 Blade Geometry

Detail	Unit	Dimension		
Tip Diameter	mm	100		
Hub Diameter	mm	48		
Hub-Tip Ratio		0.48		
Number of blade		4		
Streamline		I	II	III
Diameter	mm	48	78.43	100
β_1	deg	26.406	16.903	13.405
β_2	deg	34.09	22.50	17.998
Solidity		0.904	0.714	0.635

NUMERICAL IMPLEMENTATION

This study was carried out with a commercial Computational Fluid Dynamics (CFD) code CFX TASCflow. The three dimensional geometry of the axial flow pump impeller consisted of blade profiles, hub and shroud. The topology for mesh generation is a Generic-Single Block Grid. H-Grid is used through the blade and the flow passage. Computational grid consist of single structure block 61 nodes in the flow direction, 36 nodes from leading edge to trailing edge and 46 nodes from hub to shroud. This computational grid 101,000 (61 × 36 × 46) is applied through out the analysis.

The flow simulation is executed in the rotation frame of reference. Tubulent wall treatment, Log-Law is selected. The standard k-ε turbulence model is used. The liquid is considered incompressible while water at STP was taken as the working fluid. The volume of fluid model is selected for cavitation model. Upwind difference is used for solution scheme.

Only one flow passage is modeled because the flow is assumed to be the same in all flow passage. The boundary condition consist of two walls, inlet and outlet. At blade and hub surface, smooth relative frame stationary wall is selected as a default boundary condition. At shroud surface, relative frame counter rotating wall is applied with Log-Law wall model and smooth wall. Inlet boundary condition absolute total pressure is set include of specifacaton of turbulent intensity and length scale. Direction of absolute flow is defined in cartesian coordinate. At the outlet, a mass flow for one passage is specified. Since flow condition is replicated in each flow passage then periodic boundary condition is used.

The solver is run in steady state condition while upwind difference is selected for discretization scheme. Initial gusses of the flow field are estimated from one-dimensional analysis. Static pressure and the velocity flow field are specified as initial guess.

To compute performance characteristic curve, the simulation is run at 4 kg/s of mass flow rate and then re-run at higher mass flow rate. The interval used is 1 kg/s until the mass flow rate reach 22 kg/s. These simulations run without cavitation.

To compute head drop curve, the absolute total pressure at inflow boundary is reduced from 80000 Pa to meet the onset of cavitation. After cavitation occur the simulation is run until the inlet total pressure is reduced to 17000 Pa.

RESULTS

Several numerical simulation results are shown and used for detect formation of cavitation.

Performance Characteristic

To compute performance characteristic curve, the head rise (H) is computed from CFXTASCflow simutlation results and defined by

$$H = \frac{P_{t2} - P_{t1}}{\rho g}$$

Efficiency of axial flow impeller (η) computed by

$$\eta = \frac{\dot{m} P_{t2} - P_{t1}}{\rho M \omega}$$

where M is torque all blades.

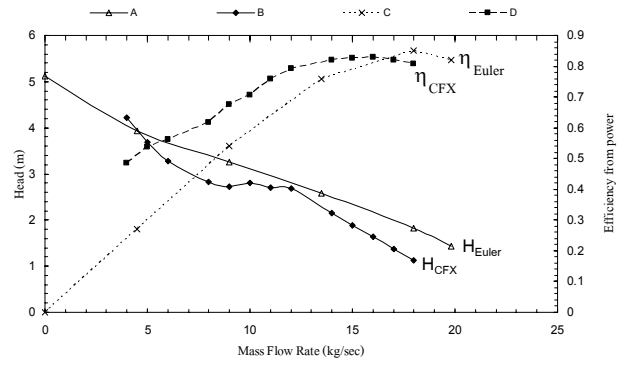


Figure 2 Axial flow pump performance characteristic curve at speed 2400 rpm, inlet total pressure 1.01325×10^5 Pa

(A) One-Dimensional Eulerian head

(B) CFXTASCflow head

(C) One-Dimensional efficiency

(D) CFXTASCflow efficiency

Figure 2 shows prediction performance characteristic which computed by CFXTASCflow and one-dimensional Eulerian performance characteristic. From the figure it can be shown that prediction head curve agreement with the one-dimensional Eulerian head curve. Below design flow, efficiency computed with CFXTASCflow departs and over efficiency computed with one-dimensional Eulerian but over design flow the efficiency CFXTASCflow prediction below efficiency computed with one-dimensional. The computational results show poor convergence when the flow is closed to shutt-off condition.

Head Drop Curve

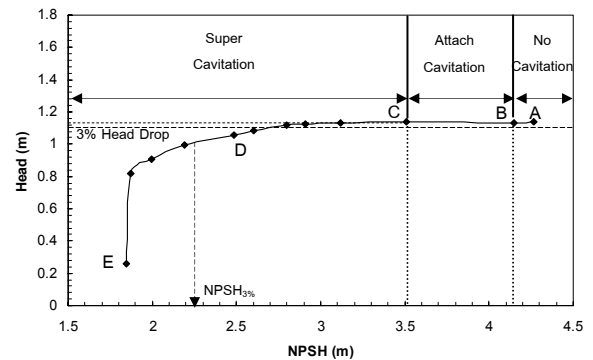


Figure 3 Head-NPSH curve at flow rate 18 kg/s and speed 2400 rpm

The NPSH value is determined by the pressure difference between the inlet pressure and the minimum pressure in the flow passage and velocity head.

$$NPSH = \frac{P_1 - P_{min}}{\rho g} + \frac{C_1^2}{2g}$$

where $C_1 = \vec{V}_{circ} + \vec{V}_{merid}$.

Figure 3 shows head drop curve as well as NPSH curve that computed by CFXTASCflow at design flow and rate speed. Volume of fluid model is selected as a cavitation model to compute rate of vapour bubble production. At inlet boundary total pressure is decreased to meet a status that cavitation formation starting. NPSH_{3%} is the value at which the head below 3% of no cavitation head. From head drop curve, predicted NPSH_{3%} can be evaluated about 2.24 m.

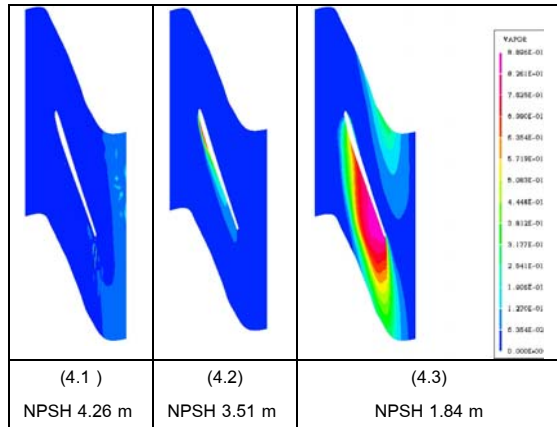


Figure 4 VAPOR Fringe Plot blade to blade view at 99% span, speed 2400 rpm and flow rate 18 kg/s

Figure 4 shows cavity length with vapor fringe plot blade to blade view which corresponds to point A, C, E respectively in head drop curve (Figure 3). There is no cavitation when NPSH = 4.26 m, attach cavitation when NPSH = 3.51 m and super cavitation when NPSH = 1.84 m as shown in figure 4. Therefore head drop curve in figure 3 can be divided according to cavity length on blade surface into three portions as no cavitation, attach cavitation and super cavitation [3]. No cavitation is range from A to B in figure 3. In this portion rate of vapor production approximate zero. Attach cavitation is range B to C that has cavity length on blade surface less than or equal chord length. Cavitation on suction surface is growing when decreasing NPSH. If cavity length grow up more than chord length, super cavitation occur as shown in figure 4.3. Super cavitation is range C to E in figure 3.

GENERATION OF VAPOR BUBBLES

To analyze inception cavitation, source term in volume of fluid model is solved. Mass exchange between vapor phase and liquid phase in cavitation zone is defined by equation (3) which depend on bubble number per unit volume and rate of change of bubble mass.

Inception Cavitation

From head drop curve showed in figure 3, NPSH value at inception cavitation that cavitation formation start can be

approximate when NPSH value is about 2.7-4.2 m. In this region, inlet total pressure in the computational model is decreased in a small interval. The result computed by CFXTASCflow shows inception cavitation form at NPSH value of 4.15 m.

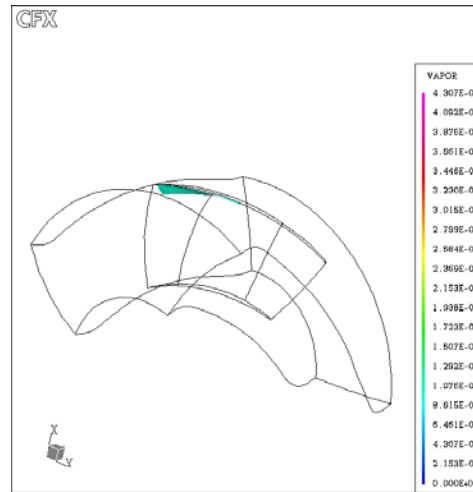


Figure 5 Inception cavitation, inlet total pressure 4.15×10^4 pascal, speed 2400 rpm (negative rotation following the right hand rule), flow rate 18 kg/s, NPSH 4.15 m, show on head drop curve with point B

Figure 5 shows inception cavitation on the area where leading edge meet the tip. Inception cavitation occurs due to flow velocity at suction side near leading edge is height, yielding flow acceleration and thus a corresponding pressure decrease below the vapor pressure level.

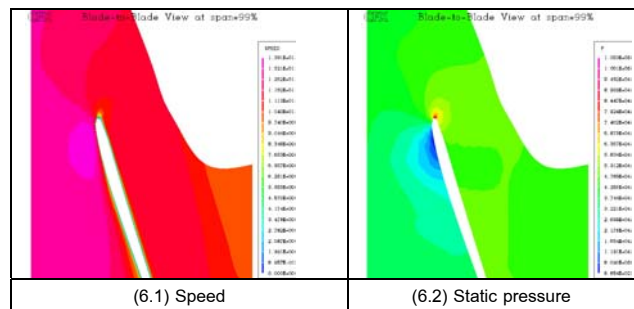


Figure 6 Fringe Plot blade to blade view at 99% span. NPSH 4.15 m speed 2400 rpm flow rate 18 kg/s

To clarify cavitation phenomena in the flow passage of an axial flow pump, the compute flow speed and static pressure is plotted in blade to blade view at NPSH value of 4.15 m that inception cavitation occurred at the blade leading edge near the tip. Figure 6.1 shows relative frame velocity that arise maximum speed near the leading edge on suction surface hence the static pressure in this region reduce below vapor pressure as shown in

figure 6.2. When the flow field static pressure decrease below liquid vapor pressure, cavitation will form.

Location of Cavitation

To describe a change in the location of cavitation while NPSH value is decreased, the predicted bubble vaporization rate in the flow passage is shown.

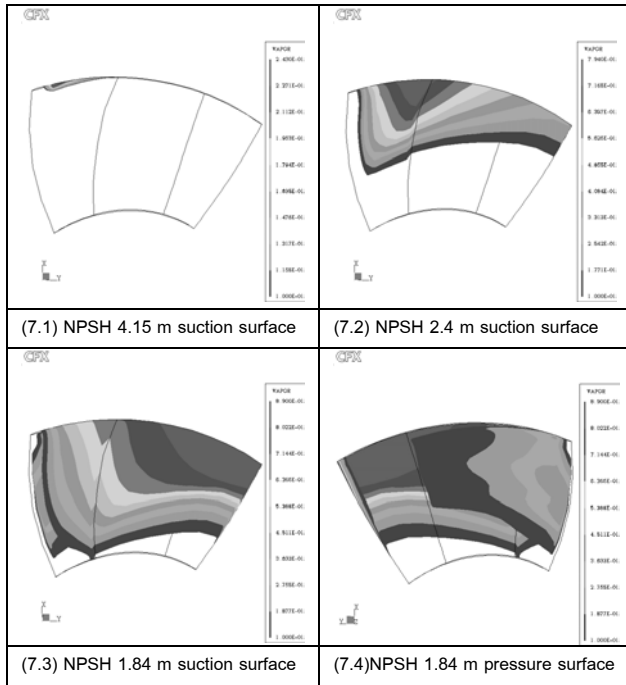


Figure 7 Fringe Plot showing cavitation on blade surface at speed 2400 rpm, flow rate 18 kg/s

Figure 7 shows VAPOR Fringe Plot with variation of NPSH. Figure 7.1 shows that the maximum evaporation rate occurred at the blade leading edge near the tip. Figure 7.2 shows that the location of maximum evaporation rate moves from the blade leading edge. Figure 7.3 shows that the maximum evaporation rates occur at the blade trailing edge near the tip. Figure 7.4 shows that cavitation occur on the pressure surface in case of super cavitation.

Hence for NPSH value lower than NPSH value that inception cavitation form, the location of maximum evaporation rate move from the blade leading edge to the blade trailing edge along the stream line near the tip.

Cavitation can be seen on pressure surface as shown in figure 7.4. If cavitation occur on pressure surface, pump head corresponding point E on head drop curve figure 3 will decrease rapidly.

CONCLUSION

Axial flow pump impeller was designed using Stephanoff design parameters on Force Vortex Theory. The flow through the blade passage was numerically studied, with commercial CFD code, CFXTASflow in order to detect formation of cavitation in pump.

The computed efficiency slight variation from one-dimensional analysis while the computed head is in good agreement with one-dimensional analysis. Head drop curve has a knee shape that head remain constant while NPSH decreased and head will be rapidly decreased at the critical point. The onset of cavitation in the blade passage can be detected and shown in quantitative and qualitative with numerical simulation. Furthermore, it can be seen that inception cavitation occur on the suction surface where the leading edge meet the tip. In case of super cavitation, cavitation zone expand to the trailing edge and occur both suction surface and pressure surface.

REFERENCES

- [1] AEA Technology Engineering Software, 2001, Theory Documentation Version 2.12, AEA Technology, pp. 311-322.
- [2] Stepanoff, A.J., 1975, Centrifugal and axial flow pumps Theory Design and Application, John Wiley, New York, pp. 138-160.
- [3] Brennen, C.E., 1994, Hydrodynamics of Pumps, Oxford University Press, London, pp. 71-96.